PB83-232025

Behavior of Constant Rate Aerosol Reactors (Journal Version)

California Univ., Los Angeles

Prepared for

Environmental Protection Agency
Research Triangle Park, NC

1982

U.S. Department of Commerce
National Technical Information Service
NTIS

TECHNICAL REPORT DATA
(Please read Instructions on the reverse before complet

1. REPORT NO. EPA-600/J-82-341	2.
3. PB83-232025	
4. TITLE AND SUBTITLE THE BEHAVIOR OF CONSTANT RATE AEROSOL REACTORS (Journal Version)	5. REPORT DATE 1982
	6. PERFORMING ORGANIZATION CODE
7. AUTHOR(S) S. K. Friedlander	8. PERFORMING ORGANIZATION REPORT NO.
9. PERFORMING ORGANIZATION NAME AND ADDRESS UCLA Department of Chemical Engineering Los Angeles, CA 90024	10. PROGRAM ELEMENT NO. CCYN1A/01-0588 (FY-83)
	11. CONTRACT/GRANT NO. Grant No. R-806404
12. SPONSORING AGENCY NAME AND ADDRESS Environmental Sciences Research Laboratory-RTP, NC Office of Research and Development U. S. Environmental Protection Agency Research Triangle Park, NC 27711	13. TYPE OF REPORT AND PERIOD COVERED
	14. SPONSORING AGENCY CODE EPA/600/09

15. SUPPLEMENTARY NOTES

REF: Aerosol Science and Technology 1:3-13 (1982)

16. ABSTRACT

An aerosol reactor is a gaseous system in which fine particles are formed by chemical reaction in either a batch or flow process. Such reactors are used to study the aerosol formation process, as in a smog reactor, or to generate a product such as a pigment or a catalytic aerosol. This paper deals with reactors in which aerosol material is generated at a constant rate. Design parameters of interest are the size distribution, number density, surface area, and mass loadings. For ideal systems composed of spherical coalescing particles, these can be predicted theoretically for certain limiting cases. However, the irregular agglomerates which may form are more difficult to characterize theoretically.

17. KEY WORDS AND DOCUMENT ANALYSIS

a. DESCRIPTORS	b. IDENTIFIERS/OPEN ENDED TERMS	c. COSATI Field/Group

18. DISTRIBUTION STATEMENT RELEASE TO PUBLIC	19. SECURITY CLASS (This Report) UNCLASSIFIED	21. NO. OF PAGES 12
	20. SECURITY CLASS (This page) UNCLASSIFIED	22. PRICE

EPA Form 2220-1 (Rev. 4-77) PREVIOUS EDITION IS OBSOLETE

REPRODUCED BY
NATIONAL TECHNICAL
INFORMATION SERVICE
U.S. DEPARTMENT OF COMMERCE
SPRINGFIELD, VA. 22161

EPA-600/J-82-341
JOURNAL ARTICLE

The Behavior of Constant Rate Aerosol Reactors

S. K. Friedlander
Department of Chemical Engineering, UCLA, Los Angeles, CA 90024

An aerosol reactor is a gaseous system in which fine particles are formed by chemical reaction in either a batch or flow process. The particle sizes of interest range from less than 10 Å (molecular clusters) to 10 μm. Such reactors may be operated to study the aerosol formation process, as in a smog reactor, or to generate a product such as a pigment or a catalytic aerosol. Aerosol reactors can be characterized by three temporal or spatial zones or regions of operation for batch and flow reactors, respectively. In zone I, chemical reaction results in the formation of condensable molecular products which nucleate and form very high concentrations of small particles. The number density depends on the concentration of preexisting aerosol. Zone II is a transition region in which the aerosol number concentration levels off as a result of hetergeneous condensation by the stable aerosol. In zone III coagulation becomes sufficiently rapid to reduce the particle number concentration. There may be a zone IV in which agglomerates form. Chemical reaction may continue to generate condensable material throughout the various zones. This paper deals with reactors in which aerosol material is generated at a constant rate. Design parameters of interest are the particle size distribution, number density, surface area, and mass loadings. For ideal systems composed of spherical coalescing particles, these can be predicted theoretically for certain limiting cases. However, the irregular agglomerates which may form in zone IV are more difficult to characterize theoretically.

INTRODUCTION

Aerosol reactors are gaseous systems in which fine particles are formed by chemical reaction either in a batch or flow process. Particle sizes range from about 10 Å to 10 μm. Such reactors may be operated in order to study aerosol formation in smog (Husar and Whitby, 1973) or to produce industrial products such as carbon black or titanium dioxide (Ulrich, 1971). Often aerosol reactors are operated unintentionally, as in the formation of flyash by the combustion of coal (Flagan and Friedlander, 1978) or the formation of lead-containing particles by the combustion of leaded gasoline in automobile engines. Photocatalytically active aerosols have been studied in a deposited form on a porous cellulose acetate film (Formenti et al., 1972).

Aerosol reactors can be operated in different modes. For example, in certain flame processes, all of the condensable material is generated over a very short period of time, after which only nucleation and coagulation take place. These can be called *pulse reactors*. In smog reactors, on the other hand, condensable material is continuously generated. These can be called *continuously reinforced reactors*. Systems operated in this mode permit the continual creation of new surface area, which is of particular interest for the production of catalytic aerosols. If the reactant concentrations and reactor temperature remain constant, the rate of formation of aerosol material is also approximately constant. The behavior of this special type of continuously reinforced reactor, the *constant rate aerosol reactor*, is the subject of this paper.

Many previous studies have been carried out with continuously reinforced aerosol batch reactors (Renzetti and Doyle, 1960; Bricard et al., 1968, 1972; Clark, 1972; Husar and Whitby, 1973; McMurry and Friedlander, 1979). The results of McMurry and Friedlander for a 65 m^3 teflon batch reactor containing SO_2, NO, and propylene are typical and are shown in Figure 1. The particle concentration rises sharply initially, reaches a peak, and then decays. The surface

Aerosol Science and Technology 1:3-13 (1982)
© 1982 Elsevier Science Publishing Co., Inc.

U.S. Government is authorized to reproduce and sell this report. Permission for furthur reproduction must be obtained from the copyright owner.

0278-6826/82/010003-11$02.75

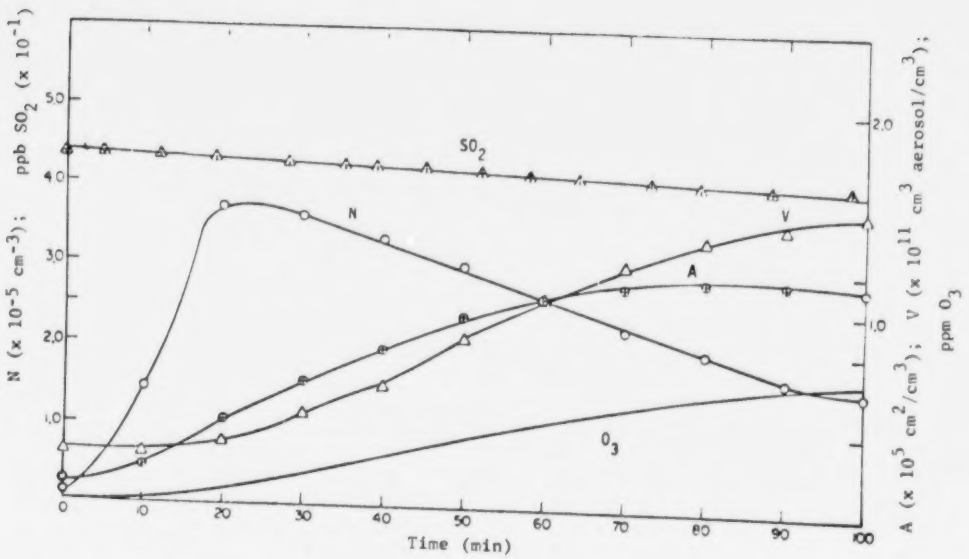

FIGURE 1. Characteristics of a continuously reinforced reactor (McMurry and Friedlander, 1979). The reactant gas mixture consisted of 43 ppb SO_2, 0.69 ppm propylene, and 1.3 ppm NO filtered air. The reactor was a Teflon film (2 mil) 65 m^3 chamber exposed to solar radiation. The figure shows an approximately constant rate of SO_2 decay leading to a steady increase in sulfuric acid aerosol of volumetric concentration V, surface area concentration A, and number density N.

area concentration increases initially and then levels off at a nearly constant concentration. The aerosol volume increases almost linearly as SO_2 reacts to form the aerosol. The measurements were made with the electrical aerosol analyzer set for a lower detectable particle size limit of 100 Å. McMurry and Friedlander also found that the presence of an aerosol in the nucleating system sharply reduces the rate of new particle formation. Tubular flow reactors have been studied by Goetz and Pueschel (1965), Kashara and Takahashi (1976), and Kasahara et al. (1980). In the studies of Takahashi and his coworkers the tubular reactor was 7.5 cm i.d. and 56.6 cm in length, and the residence time ranged from 15 to 750 sec. Kasahara et al. (1980) irradiated mixtures of SO_2, NO_2, and *trans*-2-butene and found that the particle number density N varied with residence time in a way similar to the curve of Figure 1. They also found that a preexisting aerosol significantly reduced the height of the peak.

The results of these studies are interpreted as follows: Initially, chemical reaction leads to the formation of condensable product molecules, which form new particles by self-nucleation. Over a short time scale, high concentrations of new particles form. Nucleation slows as a result of condensation on the particles and coagulation then results in the decay of the number density with time. These processes are shown schematically in Figure 2 as separate zones for a tubular flow reactor. So far the experiments have been carried out for coalescing aerosols. Figure 2 includes a final zone in which agglomerates or flocs are formed by noncoalescing aerosols.

In this paper the behavior of the constant rate aerosol reactor is discussed with a view toward the development of useful design relationships based on theory. Advances in our ability to design constant rate aerosol reactors would permit their more widespread use industrially and in laboratory research. An example of a possible new use would be their application as

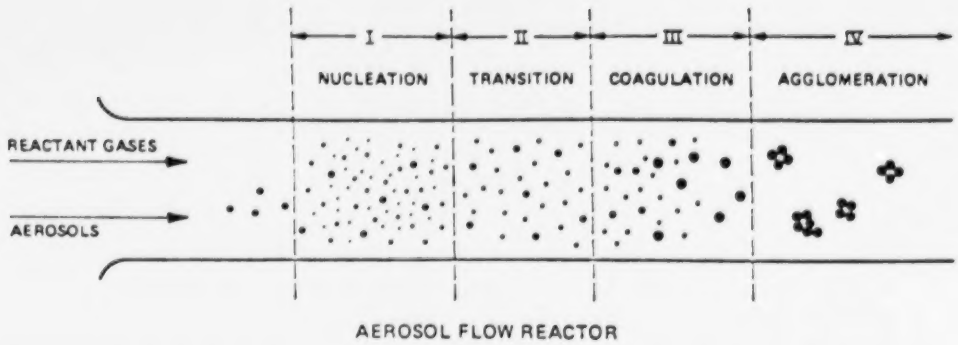

FIGURE 2. Schematic diagram of the aerosol tubular flow reactor showing the various zones corresponding to the evolution of the number density in Figure 1. Zone IV corresponds to the formation of floclike agglomerates by noncoalescing particles. This zone may follow immediately after zone I or it may not exist at all, depending on the rate of particle fusion.

catalytic flow reactors. Such systems have potential industrial importance for the following reasons:

1. By controlling the rate of the chemical reaction which produces aerosol material, the continual creation of fresh aerosol surface area is possible.
2. A smaller reactor volume for a given surface area of catalyst than for packed beds may be possible.
3. The internal resistance to diffusion of products and reactants in an aerosol floc catalyst is likely to be small.
4. Improved temperature control may be possible compared with beds of supported catalysts.

NEW PARTICLE FORMATION

The classical theory of nucleation leads to an expression for the rate of formation of critical size clusters in a particle-free gas (Frenkel, 1946; Friedlander, 1977) which can be written in the following form:

$$\bar{I} = \frac{I}{n_s^2 s_1 (kT/2\pi m_1)^{1/2}}$$

$$= \left(\frac{\pi}{6}\right)^{1/2} (g^*)^{1/6} (\ln S)^{1/2} S^2 S^{-g^*/2}, \qquad (1)$$

where

n_s is the saturation concentration of condensing molecules,

s_1 is the surface area of a monomer molecule,

k is Boltzmann's constant,

T is the absolute temperature,

m_1 is the mass of a monomer molecule,

S is the saturation ratio,

$g^* = (4\pi/3v_m)(2\sigma v_m/kT \ln S)^3$,

σ is the surface tension, and

v_m is the molecular volume.

The critical cluster size g^* is the number of monomer molecules in a particle just large enough to be stable with respect to evaporation when the saturation ratio is S.

Increasing the saturation ratio tends to reduce g^* and increase the nucleation rate. For $g^* \to 1$, the monomer can serve as the critical cluster; all collisions are successful and the process is equivalent to the coagulation of the monomer. However, the theory breaks down for small g^*, and Eq. (1) is not applicable in this limit. The theoretical predictions have been verified experimentally by Katz and his coworkers for a variety of substances (e.g., Katz et al., 1975).

If the condensable molecules are formed by chemical reaction, the rate of particle formation

(assuming a steady cluster size distribution) is given by

$$Ig^* = R. \tag{2}$$

The system is driven by a chemical reaction producing condensable monomer molecules at a rate R ($cm^{-3} s^{-1}$), which can be considered the independent variable. The saturation ratio can be calculated from Eq. (1) if R and all of the physicochemical constants appearing in Eq. (1) are known.

For a constant rate reactor, R does not change with time, and the rate of formation of clusters of size g^* is given by

$$I = R/g^*. \tag{3}$$

This simple expression holds as long as the stable clusters which have formed are not present in sufficient concentration to scavenge monomer molecules or clusters in the size range smaller than the stable clusters.

The concentration of stable particles of all sizes increases linearly with time for constant R according to the relationship

$$N(t) = Rt/g^*. \tag{4}$$

EFFECT OF SURFACE AREA ON NUCLEATION

As stable particles accumulate in the gas (or if small particles are already present), they scavenge monomer and clusters, thereby reducing the rate of formation of stable clusters. The effect of these particles on the nucleation rate can be estimated from cluster balance arguments (Friedlander, 1978, 1979). Let A be the area per unit volume of gas of existing particles (or stable clusters) and assume the thermal motion of these particles can be neglected by comparison with the smaller particles ($g < g^*$). Then the cluster balance equation takes the form

$$\frac{\partial n_g}{\partial t} = I_g - I_{g+1} - n_g \left(\frac{kT}{2\pi m_g}\right)^{1/2} A, \tag{5}$$

where n_g is the concentration of clusters containing g monomer. The particle current I_g (cm^{-3} sec^{-1}) is the excess rate at which clusters pass from the size $g-1$ by evaporation. The first two terms on the right-hand side appear in classical nucleation theory (Frenkel, 1946). The third term on the right is the loss of clusters of size g by collisions with the stable free molecule aerosol. The average cluster velocity according to kinetic theory is $(kT/2\pi m_g)^{1/2}$, where m_g is the mass of a cluster of size g.

The particle current is given by the expression

$$I_g = \beta_{g-1} s_{g-1} n_{g-1} - \alpha_g s_g n_g, \tag{6}$$

where β_{g-1} is the flux of monomer molecules to clusters of size $g-1$, α_g is the evaporative flux from clusters of size g, and s_g is the surface area of a cluster of size g. The monomer flux to a cluster of size g, based on the hard sphere model of kinetic theory for the collision frequency between clusters of size 1 and g, is given by

$$\beta_g = n_1 (kT/2\pi m_1)^{1/2} \times (1 + 1/g)^{1/2} (1 + g^{1/3})^2 s_1. \tag{7}$$

The evaporative flux is obtained by equating the collision frequency and evaporation rate at equilibrium:

$$\alpha_g = n_s (kT/2\pi m_1)^{1/2} \times (1 + 1/g)^{1/2} (1 + g^{1/3})^2 s_1. \tag{8}$$

The surface area A of stable clusters changes with time as the condensation process proceeds. However, as an approximation it can be assumed that for the cluster range $g < g^*$ a quasi-stationary state exists such that $\partial n_g/\partial t = 0$, and Eq. (5) then becomes

$$I_g = I_{g+1} + n_g (kT/2\pi m_g)^{1/2} A. \tag{9}$$

Substituting Eq. (6) in Eq. (9) gives the result

$$\beta_{g-1} n_{g-1} - \alpha_g n_g - \beta_g n_g + \alpha_{g+1} n_{g+1} - n_g (kT/2\pi m_g)^{1/2} A = 0. \tag{10}$$

On substituting Eqs. (7) and (8) in Eq. (10) the

result is

$$\tilde{n}_{g-1}\left[\frac{S[1+1/(g-1)]^{1/2}[1+(g-1)^{1/3}]^2}{(1+1/g)^{1/2}(1+g^{1/3})^2}\right] - \tilde{n}_g\left[S^{(g^*-g)^{1/3}}+S + \frac{(A/n_s s_1)}{g^{1/2}(1+1/g)^{1/2}(1+g^{1/3})^2}\right] + \tilde{n}_{g+1}\left[\frac{[1+1/(g+1)]^{1/2}[1+(g+1)^{1/3}]^2}{(1+1/g)^{1/2}(1+g^{1/3})^2} \times S^{[g^*-(g+1)]^{1/3}}\right]=0, \quad (11)$$

where $\tilde{n}_g = n_g/n_1$. The boundary conditions are the same as those of the classical theory:

$$\tilde{n}_1 = 1, \qquad \tilde{n}_G = 0 \quad (12)$$

where G represents a large value of g ($G \gg g^*$). Hence $\tilde{n}_g = f(g, S, g^*, A/n_s s_1)$. Also, by Eq. (6) the dimensionless nucleation rate is given by

$$\tilde{I}_{g^*} = \frac{I_{g^*}}{n_s^2 s_1 (kT/2\pi m_1)^{1/2}} = f[S, g^*, A/n_s s_1]. \quad (13)$$

Comparison with Eq. (1) shows that a new dimensionless group $A/n_s s_1$ has been introduced.

A numerical solution can be obtained to the linear difference Eq. (11) (Carlton, 1980). For a given value of the saturation ratio, the cluster distribution is shown in Figure 3 as a function of $A/n_s s_1$. Figure 3 shows that the cluster size distribution is very sensitive to the value of $A/n_s s_1$ for fixed S.

The rate of formation of critical clusters can be calculated from Eq. (6) with $g = g^*$. The result is shown in Figure 4 as a function of $A/n_s S_1$ for fixed S. The nucleation rate drops sharply for values of $A/n_s S_1 > \sim 10$.

The value of I_{g^*} calculated in this way could be checked experimentally if an instrument

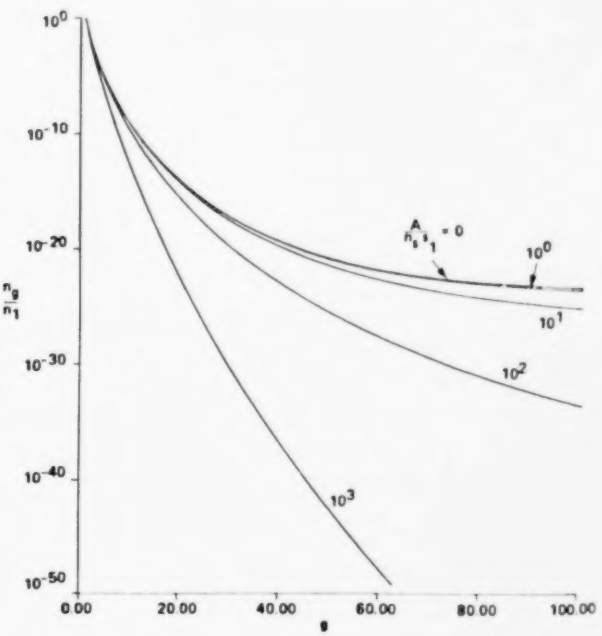

FIGURE 3. The dimensionless cluster size distribution. It is very sensitive to the surface area of existing stable particles for fixed saturation ratio and surface tension. $S = 4.0$, $g^* = 87$.

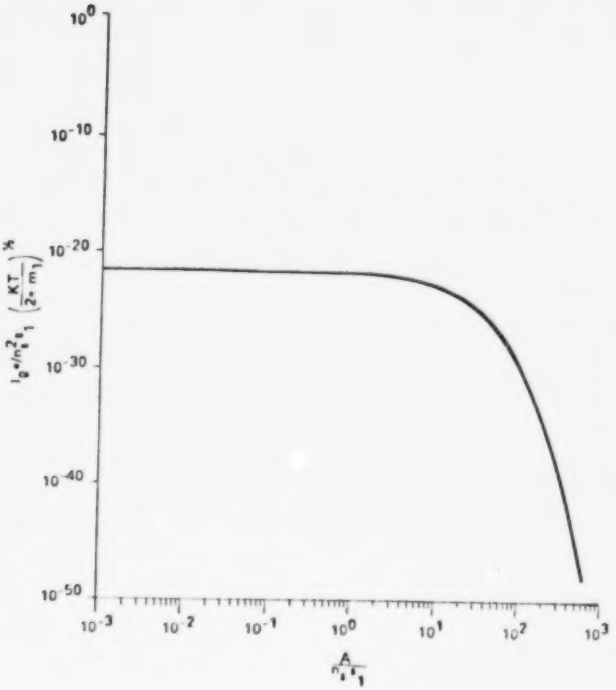

FIGURE 4. The particle current drops sharply for a fixed saturation ratio after the surface area of the foreign aerosol reaches a sufficiently large value (Carlton, 1980). $S=4.0$, $g^*=87$.

capable of detecting critical size clusters were available. Experimental studies of nucleation rates are usually carried out by optical measurement of particles which have grown large enough to be detected by the light they scatter. This corresponds to particles larger than a few tenths of a micron in diameter, much larger than the critical clusters. In the presence of a stable aerosol, the postcritical clusters can still be scavenged before they reach an optically detectable size. For this reason I_{g^*} represents the maximum value measurable by an optical detector. If no stable aerosol is present, $I_{g^*}=I$ is the value that marks entry into the optically detectable range.

TRANSITION FROM HETEROGENEOUS TO HOMOGENEOUS NUCLEATION

In classical nucleation theory, the principal independent variable is the saturation ratio. For chemically generated aerosols, the reaction rate is the natural independent variable which determines the saturation ratio and, in turn, the rate of formation of critical clusters. The reaction rate can in principle be obtained from chemical kinetic data. The saturation ratio can be eliminated from the calculation by introducing a mass balance for the monomer. In the steady state, the rate of monomer formation is related to the rates of nucleation and scavenging by the expression

$$R = I_{g^*} g^* + \sum_{g=1}^{g^*} g n_g \left[\frac{kT}{2\pi m_g}\right]^{1/2} A - n_s \left[\frac{kT}{2\pi m_1}\right]^{1/2} A, \tag{14a}$$

or nondimensionally,

$$\tilde{R} = \frac{R}{n_s^2 s_1 (kT/2\pi m_1)^{1/2}}$$

$$= \frac{I_{g^*} g^*}{n_v^2 s_1 (kT/2\pi m_1)^{1/2}}$$

$$+ \frac{A}{n_v s_1} \left[S \sum_{g=1}^{g^*} \tilde{n}_g g^{1/2} - 1 \right]. \qquad (14b)$$

Using Eq. 14(b) it is possible to eliminate the dependence of $\tilde{I}_{g^*}$ on the saturation ratio in Eq. (13) and to express it as a function of the dimensionless reaction rate parameter:

$$\tilde{I}_{g^*} = \frac{I_{g^*}}{n_v^2 s_1 (kT/2\pi m_1)^{1/2}}$$

$$= f\left(\frac{\sigma v_m^{2/3}}{kT}, \frac{R}{n_v^2 s_1 (kT/2\pi m_1)^{1/2}}, \frac{A}{n_v s_1} \right). \qquad (15)$$

The surface tension group replaces the dependence on g^*.

The mass fraction of the monomer which appears as stable particles is given by $I_{g^*} g^*/R$. This fraction can be calculated numerically from Eqs. (11) and (14b). In carrying out the calculation it is convenient to begin by assuming values for S and $\sigma v_m^{2/3}/kT$. The dimensionless nucleation rate I_{g^*} can be calculated from Eqs. (11) and (6) and the corresponding value of $\tilde{R}$ from Eq. (14b). The results of numerical calculations are shown in Figure 5 for different values of $A/n_v s_1$. Figure 5 shows that for a given value of $A/n_v s_1$ there is a critical value of the reaction rate parameter above which most of the mo-

FIGURE 5. The fraction of the monomer formed by chemical reaction which appears as new particles rises sharply when the dimensionless reaction rate reaches a critical range depending on the surface area group and the surface tension group (which is fixed for this figure).

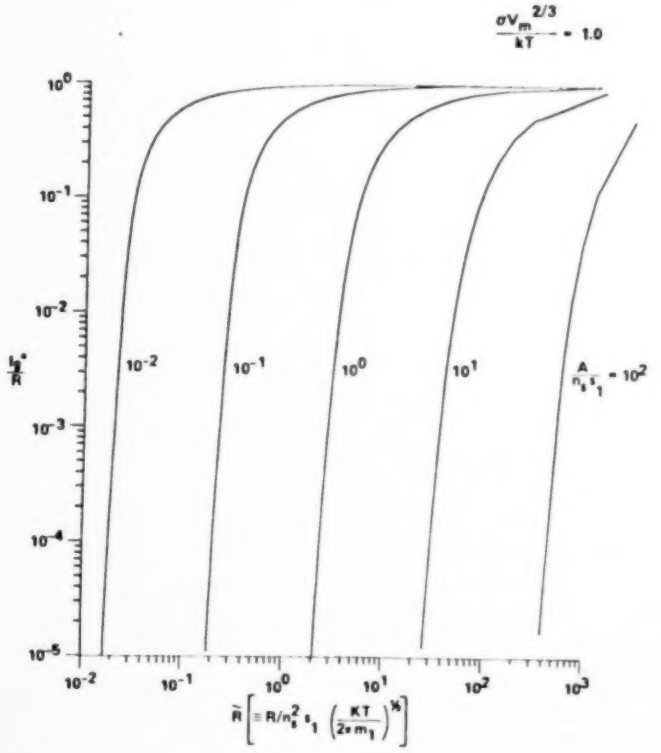

nomer appears as new particles and below which the monomer condenses on existing particles. The location of the transition zone varies with the area ratio and surface tension groups.

The path followed by a nucleating system through a constant rate flow reactor can easily be followed on Figure 5. This path is found by moving vertically downward along a given value of the (constant) reaction rate $\tilde{R}$, starting at the initial value of $\tilde{A}$. The downward path corresponds to decreasing values of $lg\ R$, the fraction of the monomer product that goes into the formation of new particles. Along the path the value of $\tilde{A}$ increases as fresh surface area is generated.

To follow the time history of this path, it would be necessary to know how the area increases with time. An analysis of this relationship is currently being conducted.

COAGULATION AND SURFACE AREA

When sufficient aerosol surface area is present (or has been generated), new particle formation ceases. The total number concentration of stable particles levels off, and the subcritical clusters are scavenged (Figure 1). This leaves an aerosol system composed of unitary particles which have accumulated during nucleation.

At some later time these stable particles begin to coagulate. The time at which this occurs depends on the collision frequency among the stable particles. Since these are large and sluggish compared with the subcritical clusters, coagulation does not become important until after the nucleation process has ended. In the coagulation zone, the condensable molecules which continue to be generated by the chemical reaction deposit directly on the existintg particles. This is true for the constant rate reactor. If the reaction rate is significantly increased, nucleation again becomes important.

For coalescing particles, self-preserving size distribution theory can be used to calculate the dynamics of the aerosol (Lai et al., 1972; Graham and Homer, 1973; Friedlander, 1977, Ch. 7). This is an asymptotic theory which holds best at times long after coagulation has begun. The theory assumes the particles are coalescing spheres which collide at a rate derived in kinetic theory for collisions between rigid elastic spheres. The resulting theoretical expression for the aerosol surface area per unit volume of gas (Lai et al., 1972) is

$$A = 2.364(\rho/kT)^{1.5}(v_m R)^{3.5} t^{1.5}, \tag{16}$$

where ρ is the particle density.

Experiment and the asymptotic theory show that the surface area per unit volume for these coalescing aerosols reaches an approximately constant value. (According to the theory [Eq. (16)] the surface area increases as $t^{1.5}$, but this dependence is too weak to test with the available experimental data.) The nearly constant value for the surface area is a result of an approximate balance between condensation, which tends to increase surface area, and coagulation, which tends to reduce the area.

FLOC FORMATION AND SURFACE AREA

The results of recent studies of pulse reactors with SiO_2 aerosols (Ulrich, 1981) could not be explained using coalescing aerosol theory because the SiO_2 particles form flocs instead of compact particles. Such flocs are of special interest for generating catalytic aerosols because they retain their large surface area. Moreover, as condensation from the gas phase continues, their surface area grows more rapidly than the surface area of a coalescing aerosol. The limiting case of the area of a noncoalescing aerosol whose individual particles remain equally accessible to condensing material can be analyzed as follows.

It is assumed that a cloud of polydisperse spherical particles is generated by homogeneous nucleation or by coagulation with rapid fusion. Beginning at $t = 0$, particles which collide stick together without fusion. They then grow by condensation of monomer molecules over their entire surface, including the points of contact with other particles. This assumption represents

a limiting case and becomes progressively poorer as the surface area increases. The dynamics of particle growth are described by the equation of continuity in particle size space (Friedlander, 1977, p. 254 ff.):

$$\frac{\partial n}{\partial t} + \frac{\partial [n d(d_p)/dt]}{\partial d_p} = 0. \tag{17}$$

Although coagulation continues during the growth process, a term for coagulation does not appear because all particles retain their identity and only growth is considered.

The particle growth law $d(d_p)/dt$ is obtained from a monomer balance on a single particle:

$$\frac{1}{v_m}\frac{d(\frac{1}{6}\pi d_p^3)}{dt} = n_1\left(\frac{kT}{2\pi m_1}\right)^{1/2}\pi d_p^2, \tag{18}$$

or

$$\frac{d(d_p)}{dt} = n_1 B, \qquad \text{where} \quad B = 2v_m\left(\frac{kT}{2\pi m_1}\right)^{1/2}.$$

For a constant rate reactor the value of n_1 decreases with time because the total surface area of the aerosol is increasing. Multiplying Eq. (17) by πd_p^3 and integrating with respect to particle size results in

$$\frac{\partial\left[\int_0^\infty \frac{1}{6}\pi d_p^3 n(d_p)\, d(d_p)\right]}{\partial t} + n_1 B\int_0^\infty \frac{1}{6}\pi d_p^3 \frac{\partial n}{\partial (d_p)}\, d(d_p) = 0 \tag{19}$$

or

$$\frac{dV}{dt} + \frac{1}{6}\pi n_1 B\left[\int_0^\infty \frac{\partial d_p^3 n}{\partial (d_p)}\, d(d_p) - 3\int_0^\infty d_p^2 n(d_p)\, d(d_p)\right] = 0. \tag{20}$$

In carrying out the integration of the second term it is assumed that n vanishes more rapidly than d_p^3 for large values of d_p. The result is

$$dV/dt = \tfrac{1}{2}n_1 BA \tag{21a}$$

or

$$n_1 = 2v_m R/AB. \tag{21b}$$

The variation of the surface area with time is found by multiplying Eq. (17) by πd_p^2 and integrating over all particle sizes. The result is

$$\frac{dA}{dt} = \frac{4\pi v_m R}{A}\int_0^\infty n d_p\, d(d_p). \tag{22}$$

The integral on the right-hand side is obtained by multiplying both sides of Eq. (17) by d_p and integrating over particle size:

$$d\left[\int_0^\infty n d_p\, d(d_p)\right]\Big/ dt = 2v_m RN/A. \tag{23}$$

In the case of a noncoalescing aerosol the total number density N of the original particles is constant.

Taking the derivative of Eq. (22) with respect to time and substituting Eqs. (21b) and (23) produces

$$A\frac{d[A\, dA/dt]}{dt} = 8\pi(v_m R)^2 N = C. \tag{24}$$

To integrate, let $w = dA/dt$. Susbstitution in Eq. (24) then gives

$$(Aw)\, d(Aw) = C\, dA. \tag{25}$$

Integrating gives

$$\tfrac{1}{2}(Aw)^2 = CA + C_0, \tag{26}$$

where C_0 is a constant of integration. Taking the square root of both sides, one obtains

$$\frac{A}{\sqrt{2}}\frac{dA}{dt} = (CA + C_0)^{1/2}. \tag{27}$$

Integrating

$$\int \frac{A\,dA}{(CA+C_0)^{1/2}} = \int \sqrt{2}\,dt \tag{28}$$

gives the result

$$(2/C^2)[\tfrac{1}{3}(CA+C_0)^{3/2} - C_0(CA+C_0)^{1/2}] = \sqrt{2}t + C_1. \tag{29}$$

The constants C_0 and C_1 can be evaluated from the initial conditions $A = A_0$ and $dA/dt = (dA/dt)_0$ at $t = 0$. The value of $dA/dt = (dA/dt)_0$ can be obtained from Eq. (22) and is given by

$$\left(\frac{dA}{dt}\right)_0 = \frac{4\pi v_m R N \bar{d}_{p0}}{A_0}, \tag{30}$$

where $\bar{d}_{p0}$ is the average particle diameter at $t = 0$.

For sufficiently large values of t (and A), Eq. (29) shows that A is given by the relation

$$A \to (6)^{2/3}\pi^{1/3}(v_m R)^{2/3}N^{1/3}t^{2/3} \quad (A \gg A_0). \tag{31}$$

Thus for noncoalescing particles the aerosol surface area for the constant rate reactor increases at $t^{2/3}$, much faster than the surface area of the coalescing aerosol, which increases at $t^{1/3}$. This result holds for particles which continue to grow by molecular deposition over all of their surface, including points of contact with other particles composing the agglomerates (flocs). Thus it represents the maximum area attainable by the system. The actual area would be expected to fall between the results for coalescing and noncoalescing particles.

The mechanisms of particle fusion in sintering have been examined by Kingery and Berg (1955). They considered

1. viscous flow under the influence of surface tension,
2. evaporation–condensation of material at the particle juncture, and
3. diffusional processes, either surface of volume.

Mechanisms such as these must be incorporated within coagulation theory to permit calculation of the total surface area. An approximate method for carrying out such calculations for the viscous flow surface tension mechanism has been proposed by Ulrich and Subramanian (1977). They assumed that a single primary particle is in contact with several other primary particles, thus creating a cell within the floc, and calculated the rate of fusion of the contacting particles. It would be of interest to apply such models to the constant rate aerosol flow reactor in which condensation takes place along with coagulation.

SUMMARY

If condensable monomer molecules form in a gas by chemical reaction, nucleation occurs after monomer concentrations have reached a sufficiently high level. When the monomer molecules are produced at a constant rate, a steady state is eventually reached in which the rate of particle formation is given by

$$I = R/g^*.$$

The accumulation of stable particles in the gas eventually suppresses nucleation by scavenging of monomer and clusters. This results in a transition from homogeneous to heterogeneous nucleation. Reaction rate can be regarded as an independent parameter which drives the nucleation process. The transition from homogeneous to heterogeneous nucleation occurs at a reaction rate determined by the surface area of stable particles and a dimensionless surface tension group.

After heterogeneous nucleation has begun, the concentration of stable particles levels off until, at a somewhat later time (or position downstream), coagulation takes over. Coagulation causes the particle concentration to decrease, and the total surface area levels off for coalescing particles with continuing monomer condensation.

If the rate of particle fusion is slow, flocs form and the aerosol surface area increases with time as condensation of monomer continues on the particles. Such flocs are difficult to characterize because the mechanisms and rate of particle fusion are not well understood.

This work was supported in part by EPA grant No. R-806404 and by a grant from the Ford Motor Company. The contents do not necessarily reflect the views and policies of the Environmental Protection Agency.

REFERENCES

Bricard, J., Billiard, F., and Madelaine, G. (1968). Formation and evolution of nuclei of condensation that appear in air initially free of aerosols, *J. Geophys. Res.* 73:4487–4496.

Bricard, J., Cabane, M., Madelaine, G., and Vigla, D. (1972). Formation and properties of neutral ultrafine particles and small ions conditioned by gaseous impurities of the air, *J. Colloid Interface Sci.* 39:42–58.

Carlton, G. N. (1980). Predicting new particle formation from preexisting aerosol concentration, M.S. thesis, University of California, Los Angeles.

Clark, W. E. (1972). Measurements of aerosols produced by the photochemical oxidation of SO_2 in air, Particle Technology Lab. Publ. No. 181, University of Minnesota.

Flagan, R. C., and Friedlander, S. K. (1978). Particle formation in pulverized coal combustion—a review, in *Recent Developments in Aerosol Science* (Shaw, D.T., ed.), Wiley-Interscience, New York, pp. 25–29.

Formenti, M., Juillet, F., Meriaudeau, P., Teichner, S. J., and Vergnon, P. (1972). Preparation in a hydrogen–oxygen flame of ultrafine metal oxide particles, *J. Colloid Interface Sci.* 39:79–89.

Frenkel, J. (1946). *Kinetic Theory of Liquids*. Dover, New York (2nd ed., 1955), pp. 390–400.

Friedlander, S. K. (1977). *Smoke Dust and Haze*, Wiley–Interscience, New York.

Friedlander, S. K. (1978). A note on new particle formation in the presence of an aerosol, *J. Colloid Interface Sci.* 67:387–388.

Friedlander, S. K. (1979). Future aerosols of the southwest: Implications for fundamental research, *Ann. NY Acad. Sci.* 338:588–598.

Goetz, A., and Pueschel, R. F. (1965). The effect of nucleating particles on photochemical aerosol formation, *J. Air Pollut. Control Assoc.* 15:90–95.

Graham, S. C., and Homer, J. B. (1973). Coagulation of molten lead aerosols, Faraday Symp. of the Chemical Society No. 7, pp. 85–96.

Husar, R. B., and Whitby, K. T. (1973). Growth mechanisms and size distributions of photochemical aerosols, *Environ. Sci. Technol.* 7:241–247.

Kasahara, M., and Takahashi, K. (1976). Experimental studies on aerosol particle formation by sulfur dioxide, *Atmos. Environ.* 10:475–486.

Kasahara, M., Takahashi, K., and Tohno, S. (1980). Photochemical aerosol formation in multi-component systems containing preexisting particles, in *Atmospheric Pollution 1980 Proceedings of the 14th International Colloquium* (Benarie, M. M., ed.), Elsevier, Amsterdam.

Katz, J. L., Scoppa, C. J., Kumar, N. G., and Mirabel, P. (1975). Condensation of a supersaturated vapor part II—homogeneous nucleation of normal-akyl benzenes, *J. Chem. Phys.* 62:448.

Kingery, W. D., and Berg, M. (1955). Study of the initial stages of sintering solids by viscous flow, evaporation–condensation and self-diffusion, *J. Appl. Phys.* 26:1205–1212.

Lai, F. S., Friedlander, S. K., Pich, J., and Hidy, G. M. (1972). The self-preserving particle size distribution for Browian coagulation in the free-molecule regime, *J. Colloid Interface Sci.* 39:395–405.

McMurry, P. H., and Friedlander, S. K. (1979). Aerosol formation in reacting gases: Relation of surface area to rate of gas-to-particle conversion, *J. Colloid Interface Sci.* 64:248–257.

Renzetti, N. A., and Doyle, G. J. (1960). Photochemical aerosol formation in sulfur dioxide-hydrocarbon systems, *Int. J. Air Pollut.* 2:327–345.

Ulrich, G. D. (1971). Theory of particle formation and growth in oxide synthesis flames, *Combust. Sci. Technol.* 4:47–57.

Ulrich, G. D., and Subramanian, N. S. (1977). Particle growth in flames III. coalescence as a rate-controlling process, *Combust. Sci. Technol.* 17:119–126.

Ulrich, G. D. (1981). Aggregation and growth of submicron oxide particles in flames, presented at the ACS IEC Symp., Tucson, AZ, January 1981.